

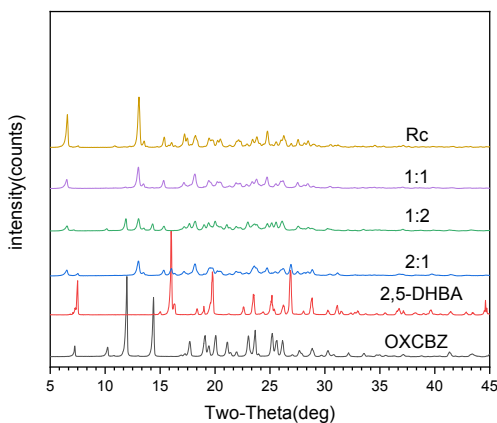
Supporting Information

Investigating solubilization effect of oxcarbazepine by forming cocrystals

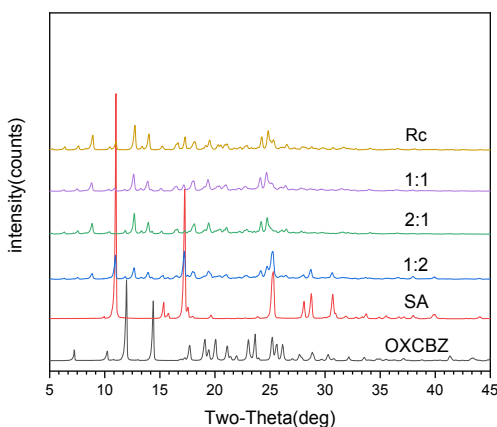
Xiangrong Li,^a Guojia Yu,^a Xinjian Chen,^a Lichao He,^a Zhiyong Zhou^{*a} and Zhongqi Ren^{*a}

^aCollege of Chemical Engineering, Beijing University of Chemical Technology, Beijing 100029, People's Republic of China

Corresponding author: renzq@mail.buct.edu.cn (Zhongqi Ren); Tel: (+86)-10-64433872;
zhouzy@mail.buct.edu.cn (Zhiyong Zhou)

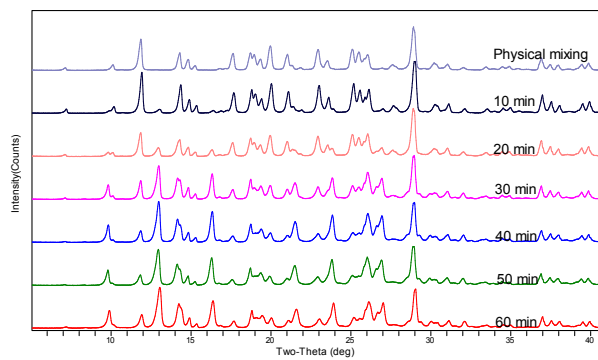


(a)

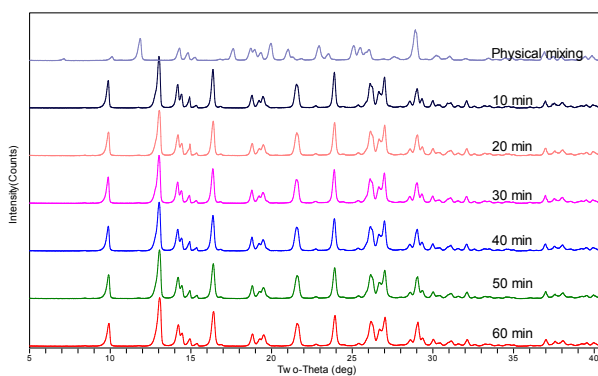


(b)

Fig. S1 PXRD patterns of co-crystals (a) OXCZBZ-2,5-DHBA and (b) OXCZBZ-SA.

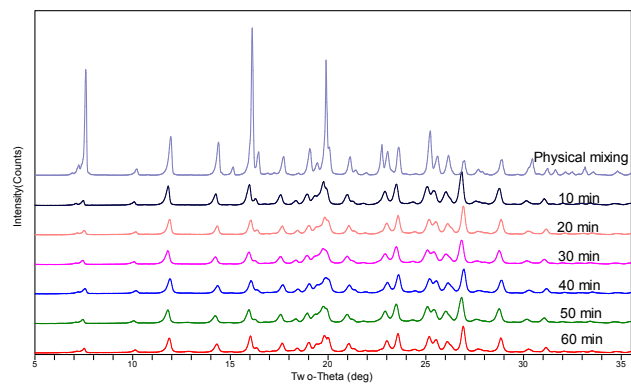


(a)

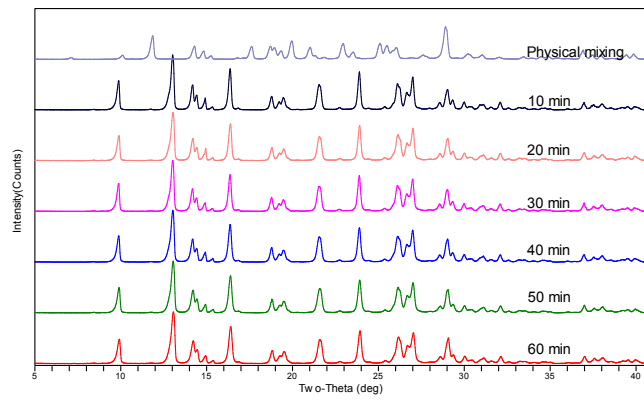


(b)

Fig. S2 PXR D patterns of OXC BZ-OA cocrystals formed by different methods. (a) grinding by NG and (b) grinding by LAG.

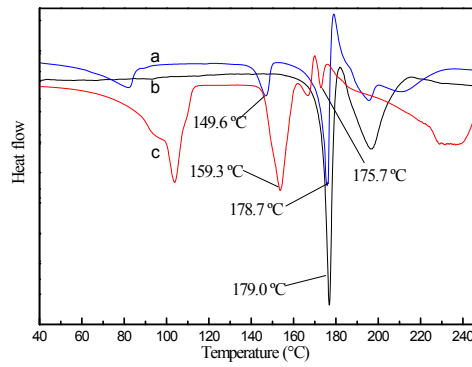


(a)

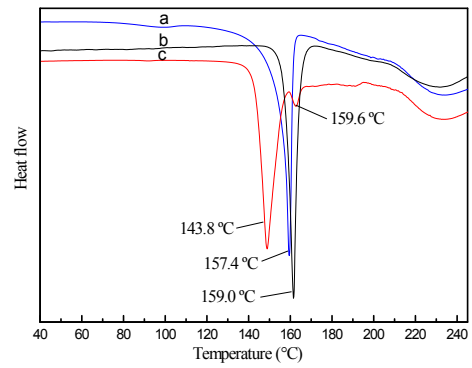


(b)

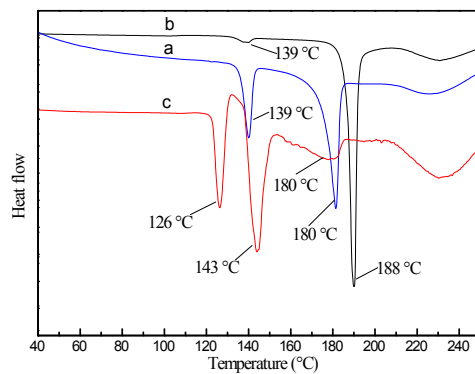
Fig. S3 PXR D patterns of OXC BZ-2,5-DHBA cocrystals formed by different methods. (a) grinding by NG and (b) grinding by LAG.



OXC BZ-OA



OXC BZ-2,5-DBHA



OXCZBZ-SA

Fig. S4 DSC curves of cocrystals formed under different conditions. (a) LAG, (b) RC and (c) physical mixing.

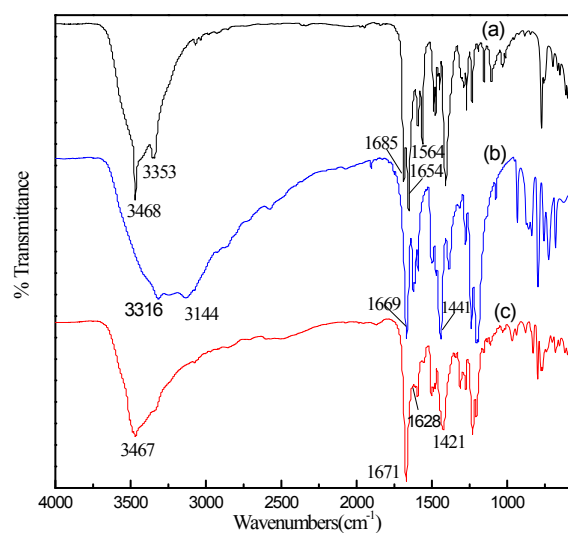


Fig. S5 FT-IR spectra of OXCZBZ and its cocrystal. (a) OXCZBZ, (b) 2,5-DHBA and (c) OXCZBZ-2,5-DHBA cocrystal.

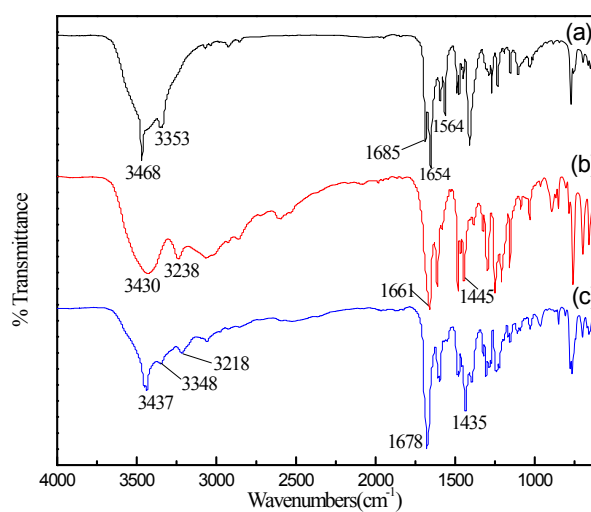


Fig. S6 FT-IR spectra of OXCZBZ and its cocrystals (a) OXCZBZ, (b) SA and (c) OXCZBZ-SA cocrystal.

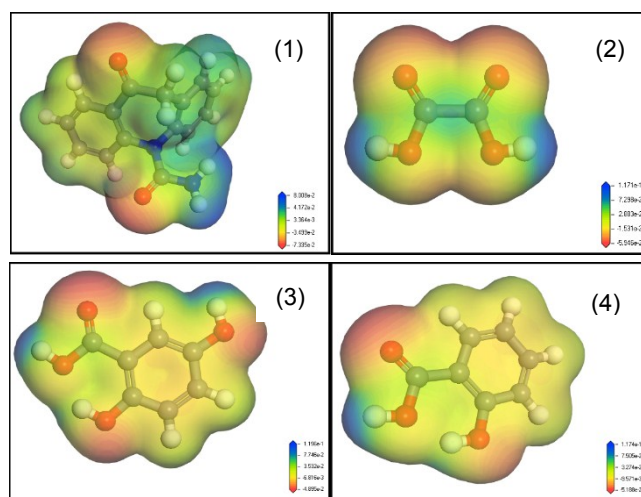


Fig. S7 Surface electrostatic potentials of (1) OXCBBZ, (2) OA, (3) 2,5-DHBA and (4) SA.

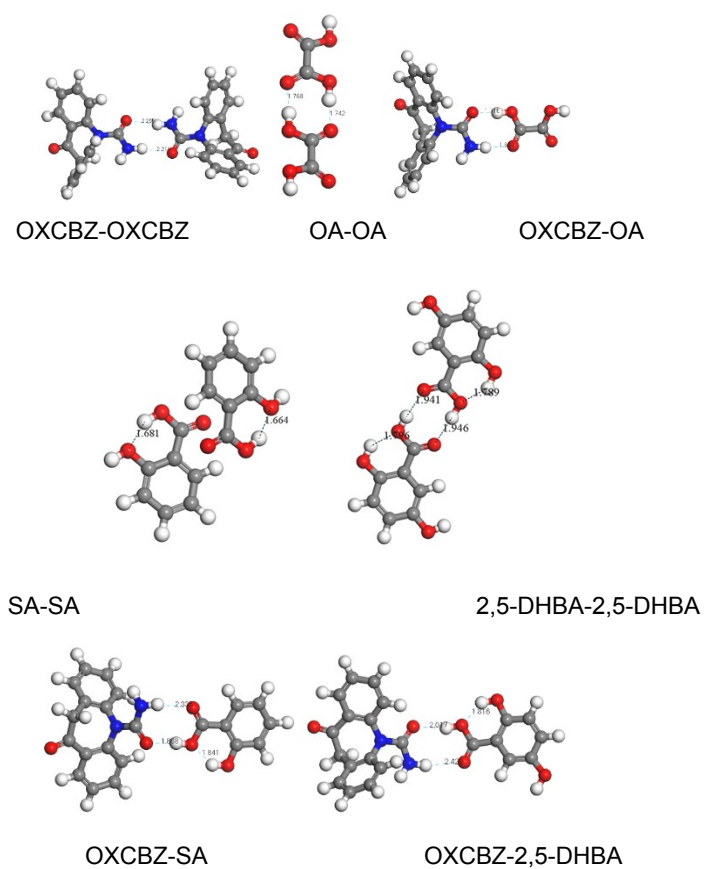
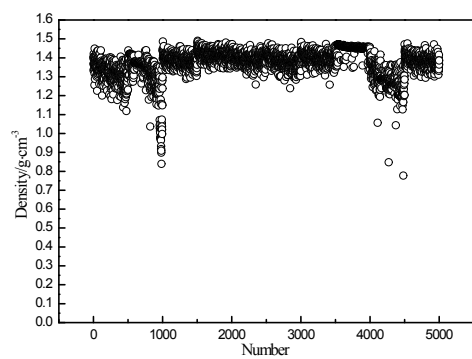
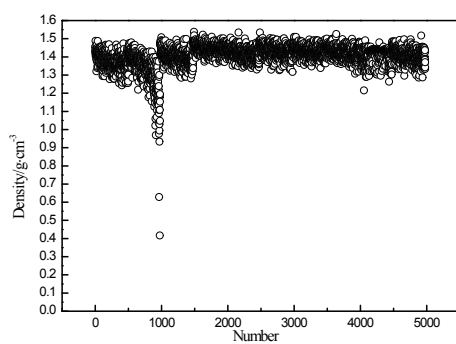


Fig. S8 Geometric structure diagrams after the basic group optimization.



(a)



(b)

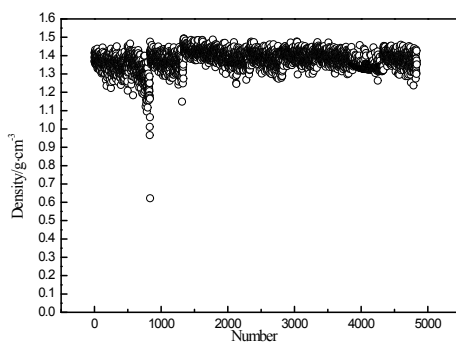
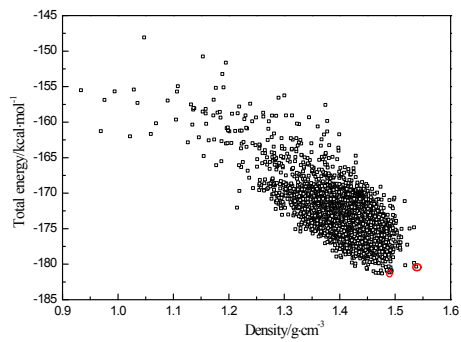
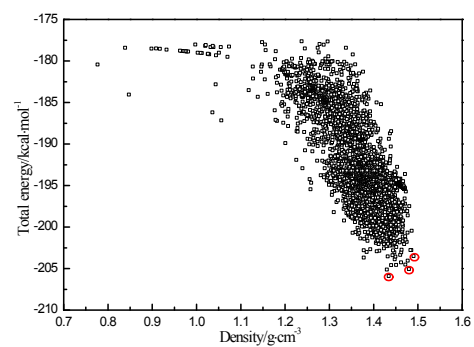


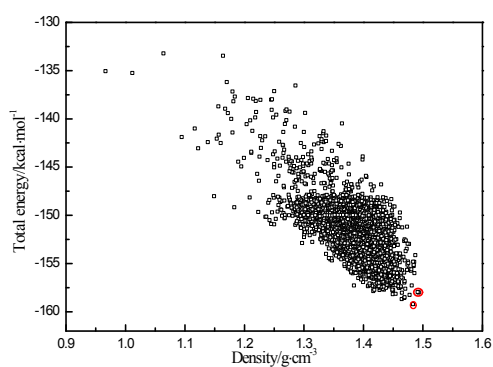
Fig. S9 Density distribution of cocrystals (a) OXCZBZ-OA cocrystal, (b) OXCZBZ-2,5-DHBA cocrystal and (c) OXCZBZ-SA cocrystal.



(a)



(b)



(c)

Fig. S10 Energy and density distributions of cocrystals (a) OXCZ-2,5-DHBA, (b) OXCZ-OA and (c) OXCZ-SA.

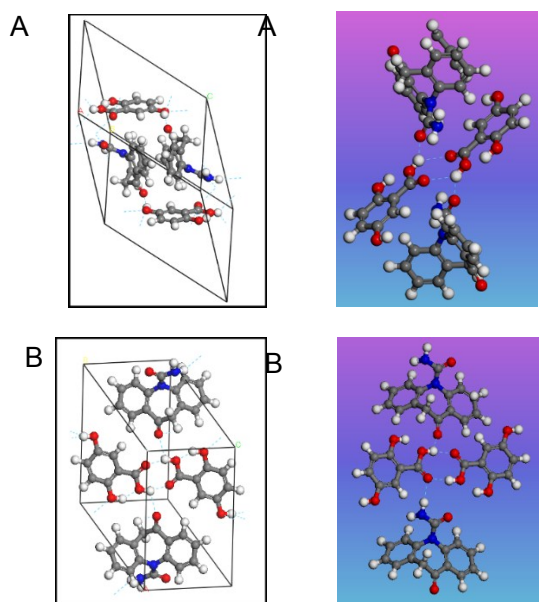


Fig. S11 Molecular arrangement (left) and H bond position (right) in Unit Cell of OXCZ-2,5-DHBA cocrystal (A and B correspond to P-1 and P-1 space groups in Table 5, respectively).

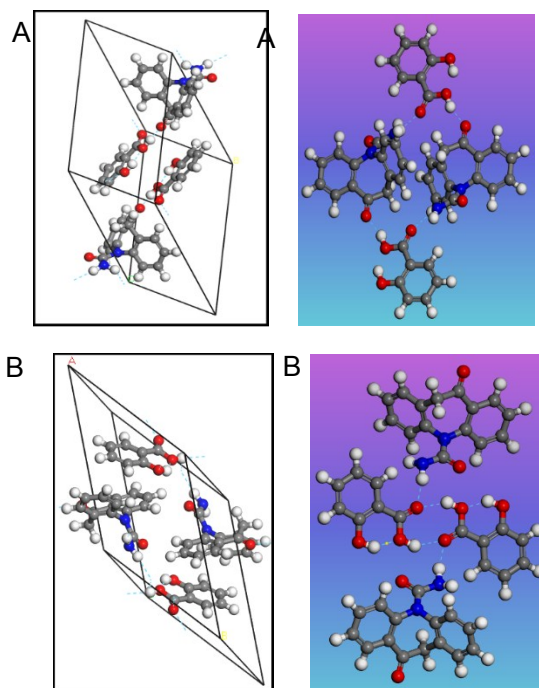
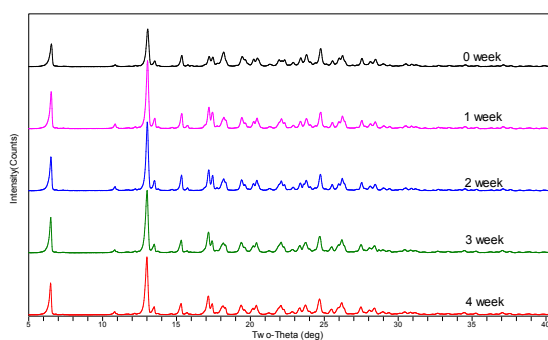
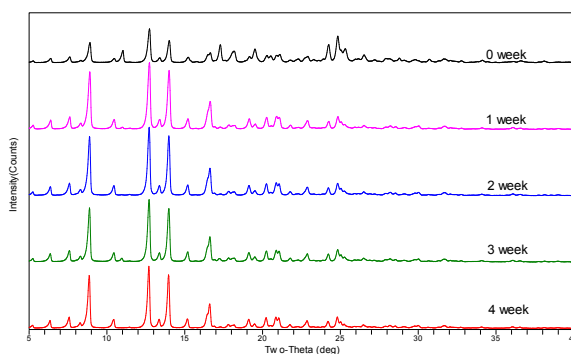


Fig. S12 Molecular arrangement (left) and H bond position (right) in Unit Cell of OXCBZ-SA cocrystal (A and B correspond to P-1 and P-1 space groups in Table 5, respectively).

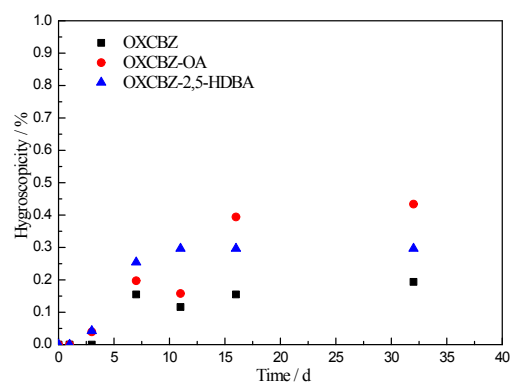


(a)

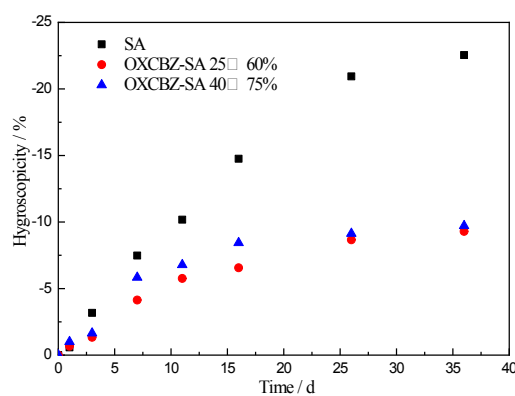


(b)

Fig. S13. PXRD patterns of cocrystals at 40 °C and different times under 75% RH. (a) OXCBZ-2,5-DHBA cocrystal and (b) OXCBZ-SA cocrystal.



(a) OXCZ, OXCZ -OA, and OXCZ -2,5-DHBA cocrystal at 40 °C, 75% RH



(b) SA and OXCZ -SA cocrystal at 25 °C, 60% RH and 40 °C, 75% RH

Fig. S14. Moisture absorption rates of OXCZ and its cocrystals.

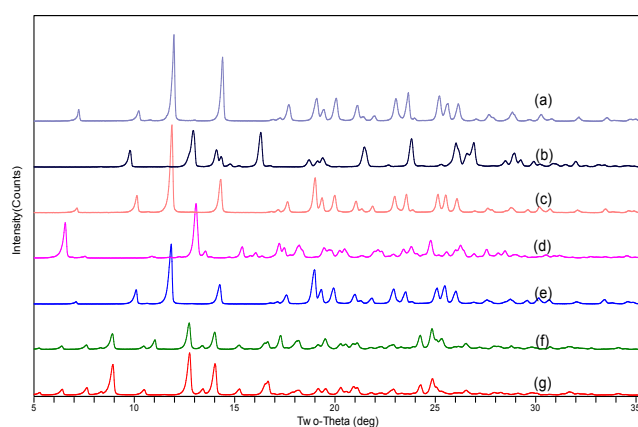


Fig. S15 PXR D patterns of remaining solid after dissolution of OXCZ and its cocrystals. (a) OXCZ, (b) OXCZ-OA, (c) OXCZ-OA after dissolution, (d) OXCZ-2,5-DHBA, (e) OXCZ-2,5-DHBA after dissolution, (f) OXCZ-SA and (g) OXCZ-SA after dissolution.